IJASRM
International Journal of Advanced Scientific Research and Management, Volume 4 Issue 5, May 2019
www.ijasrm.com
ISSN 2455-6378

Newly Developed Eco-friendly Bio-based Polyurethane Coating for Enhanced Materials Properties for Outer Structure Applications in Aeronautical Industries

Abhishek Chandramohan[1] and Prashaant Chandramohan[1]

[1] VPA Laboratory Private Limited,
Chennai, Tamil Nadu, 600045, India

Abstract

The advancements in thin film applications has given rise to many possibilities in chemical industries. In turn, these new products also finds its purpose as protective coatings. With specific functional groups, it is possible to synthesize polymers based on individual requirements. One of the recent trends in research is the use of bio-based coatings as replacements for paints. The goal is not only to be more eco-friendly but also to improve specific material properties such as flame retardation, resistance to corrosion, improved viscoelasticity, electrical conductivity, resistance against rupture and etc. In this research, an environmental-friendly non-isocyanate polyurethane coating was prepared such that it has resistance to ultraviolet radiations. This was achieved by introducing fine silicon dioxide powder at final stages of the composite preparation. Hence, materials characterization and mechanical properties of the composite were studied to understand the failure mechanism of the multilayers.

Keywords: *Non-isocyanate polyurethane (NIPU); Polymer coating; Materials characterization; Fatigue.*

1. Introduction

The stringent requirements in aviation industries extends to environment as well, where replacing harmful substances during production or use of products are mandated. Although the unfriendly components to the environment are not yet completely replaced, recent research shows many possibilities. One such progress is replacing paints with organic coatings. Paints are synthetic compounds which contains toxic elements. Whereas, organic coatings are synthesized through green routes which makes it completely bio-based and eco-friendly. Such bio-sourced polymers has short gel time, better stability with chemical and thermal facets and also with hydroxyl groups, which signifies better degradation process [1, 2]. In addition to that, organic polymers has better resistance against corrosion and failure mechanisms since it is amorphous i.e., viscoelastic. The ease in functional formulation of organic polymers favours in tailor-making a compound where specific materials properties can be improved. In this work, non-isocyanate polyurethanes (NIPU) were used as the polymer coating because unlike conventional polyurethanes that are extremely popular in coating applications, NIPUs can be synthesized without solvents or isocyanates. This effectively makes the compound environmental-friendly.

In a metal-polymer composite, an intermediate layer is necessary to act as a bonding layer for metal and polymer to form a proper interface, particularly if the metal is untreated. Studies on such interactions provides information on morphology and mechanical properties of the composite. The intermediate layer which bonds the polymer and metal with respect to this system is deposition, which is an essential part because the aluminium (Al) alloy used here is uncladded 2024 T3 grade. Uncladded metal and bio-sourced polymers are adopted in this work because the goal is to create a more eco-friendly material by eliminating the use of extensive toxic chemicals during synthesis.

Staying true to the objective, the depositions were synthesized from plasma techniques. The advantage of plasma deposition over anodization is that any side of the metal can be easily deposited. In addition to that, the precursors used in plasma depositions can also be bio-sourced. This is in stark contrast with anodization, where acid bath is necessary to force a rough surface. Moreover, the

IJASRM
International Journal of Advanced Scientific Research and Management, Volume 4 Issue 5, May 2019
www.ijasrm.com
ISSN 2455-6378

precursors in plasma deposition can be easily modified to obtain the desired thickness or morphology of the layer.

2. Synthesis of Composite

The plasma depositions on uncladded Al 2024 T3 were made similar to the techniques demonstrated by Reniers et al. [3]. Atmospheric plasma coatings by low-pressure chemical vapour deposition in ambient conditions were performed, where methacrylate anhydride with helium deposition were deposited over the Al plate of 1 mm thickness on both sides. Since the goal is towards creating an eco-friendly compound, no post-treatments were performed. The resulting thickness of the plasma deposition was 25 nm. Subsequently, NIPU was bar-coated on top of the plasma deposition at 100 µm thickness. The polymer coating is strongly adhered to the plasma deposition because the porous surface by deposition helps achieve strong mechanical adhesion. The polymers were prepared similar to the techniques demonstrated by Tryznowski et al. [4]. Here, bis(cyclic carbonate) 2 was synthesized by polyaddition of poly(cyclic carbonate)s. Along with diamines, bis(cyclic carbonate) 2 was used as monomer in the preparation of NIPU. Immediately after the polymer coating, fine silicon dioxide (SiO_2) powder of 99.5% were dusted on top. The goal here is to create a thin top surface that can protect the polymer from ultraviolet (UV) radiations and also allow breathing for the compound while curing at room temperature. The final product (Fig. 1) is obtained in such a way that it would replace the paints but also has resistance to UV radiations.

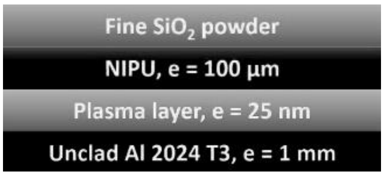

Fig. 1. Schematic of multilayers

3. Materials Characterization

Surface observations were made under focused ion beam (FIB) scanning electron microscope (SEM) where the average size of pores in plasma coating were 7 µm (Fig. 2), which improves the bonding with polymer layers by forcing mechanical adhesion. In order to study the plasma deposition, FIB cuts of the size 6 µm x 15 µm x 0.1 µm were made. These were in turn observed under transmission electron microscope (TEM). Al alloy had notable presence of copper precipitates (Fig. 3.A), which were confirmed by dispersion experiment. Whereas, the dark spots in Al alloys (Fig. 3.A) signifies dislocations in the crystal structure [5]. The thickness of the amorphous plasma layer was 25 nm (Fig. 3.A) and upon a closer look at the interface, there seems to be effective bonding with Al. From energy-dispersive X-ray spectroscopy (EDX) experiment in TEM (Fig. 4.A), various elements were observed. These elements were found to be plasma compositions, which were confirmed by X-ray fluorescence (XRF) experiment (Fig. 4.B). At the interface (Fig. 3.B), the presence of compounds from either side of the layers were observed, which was due to the decomposition of the Al surface during plasma deposition i.e., hot blast. This signifies effective interaction between Al and plasma deposition at the interface since cohesion is important in multilayers for good structural integrity of the composite. If the mechanical adhesion is not effective, then the layer scales away during failure mechanisms.

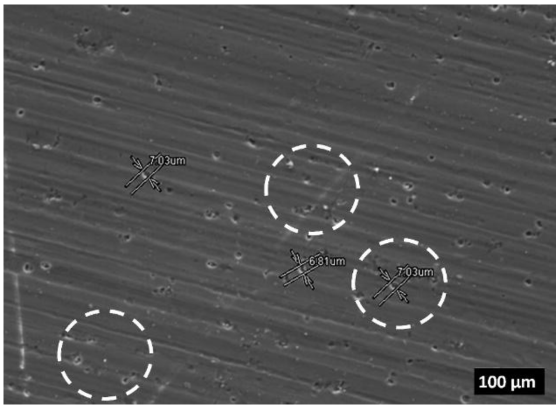

Fig. 2. Porosity of plasma deposition under FIB SEM

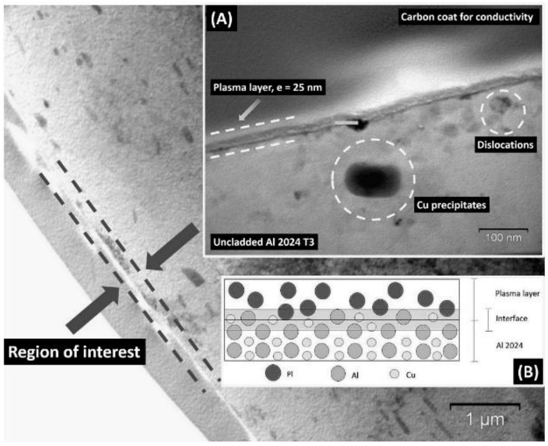

Fig. 3.(A). TEM observation of Al alloy and plasma deposition and, (B). Schematic of Al alloy-Plasma deposition interface

ISSN 2455-6378

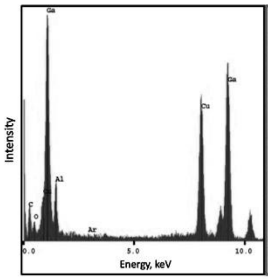

(A)

Compound Formula	nZ	Concentration weight %	Line 1	Stat. Dev. 1	Depth 1
Al	13	86.29	Al KA1-HR-Min	0.038	11 um
O	8	6.75	O KA1	0.12	1,4 um
Cu	29	4.159	Cu KA1-HR-Min	0.0017	0,17 mm
Mg	12	1.751	Mg KA1-HR-Min	0.0066	7,6 um
Mn	25	0.504	Mn KA1-HR-Min	0.0033	71 um
Fe	26	0.21	Fe KA1-HR-Min	0.0017	90 um
Si	14	0.167	Si KA1-HR-Min	0.0062	2,7 um
Zn	30	0.0836	Zn KA1-HR-Min	0.00069	0,21 mm
Ti	22	0.019	Ti KA1-HR-Min	0.0012	33 um
Cl	17	0.014	Cl KA1-HR-Min	0.0017	7,6 um
Cr	24	0.011	Cr KA1-HR-Min	0.00085	56 um
Ca	20	0.011	Ca KA1-HR-Min	0.0013	19 um
Ga	31	0.0084	Ga KA1-HR-Min	0.00036	0,20 mm
V	23	0.0077	V KA1-HR-Min	0.00082	43 um
S	16	0.0074	S KA1-HR-Min	0.0011	5,4 um
Zr	40	0.00501	Zr KA1-HR-Min	0.00019	0,92 mm
Ni	28	0.0031	Ni KA1-HR-Min	0.00032	0,14 mm
P	15	0.0025	P KA1-HR-Min	0.0013	3,8 um
Total wt%		100.0			

(B)

Fig. 4.(A). TEM EDX of Al alloy-Plasma deposition interface and, (B). XRF of plasma deposition

4. Experiment

To model and ultimately guide the selected system, it is important to conduct experimental study because the question of breaking strength is essential to maintain the protective feature of the coating. In such cases, fatigue tests are suitable because of cyclic loading, where crack resistance can be observed. This is expressed by Paris' law [6]. The principles of fracture mechanics helps in predicting the number of cycles (N) spent on crack growth either for a specified range or till failure. Crack growth rate (da/dN) is defined as the extension of crack in each cycle. Hence, the fail-safe design approach is commonly used to predict the fatigue life in structures.

$$\frac{da}{dN} = C\Delta K^n$$

Where a = crack length, c and n = material constants and ΔK (K_{max} – K_{min}) = range of stress intensity factor.

5. Results and Discussions

The composite was tested using servo-hydraulic machine at room temperature with load ratio, R (K_{min} / K_{max}) of 0.1, which was held constant to keep smooth governing of tensile stress. In fracture mechanics, the damage which causes the growth in crack tip is governed by variations in local elastic-plastic field during the cycle. da/dN is obtained by the slope of crack growth at 'a'. The fatigue crack growth rate curve (Fig. 5) is divided into three stages:

Stage 1:

Non-continuum behaviour of the material is represented in this region, which is largely influenced by microstructure and mean stress (σ_{mean}). The threshold stress intensity factor (ΔK_{th}) is where the fatigue crack growth is too small to measure, which depends on the frequency of loading. ΔK_{th} (Fig. 5) is useful in designing a component that is subjected to low stress levels and very high N. The theory in crack mechanisms states that the fatigue cracks are initiated on the free surface, which forms initial slip lines leading to a cyclic mechanism that builds up the ridges as it tends to increase over the range, where the crack takes the direction normal to the maximum tensile stress (σ_{max}). Here, the point of transition from stage 1 to stage 2 depends on σ_{max}.

Stage 2:

In a da/dN curve, stage 2 (Fig. 5) is generally the largest that is linear with slope, where fatigue crack growth life representing stable da/dN is determined. This region represents the continuum behaviour that is largely influenced by frequency, where linear elastic behaviour of the material is associated. The point of transition from stage 2 to stage 3 depends on yield strength (σ_{ys}), K and R.

Stage 3:

ΔK is high in the final stage, which signifies high da/dN with low fatigue life. This region represents the static behaviour largely influenced by the thickness of the material, which is characterized by rapid unstable crack growth till failure (Fig. 5). In practical engineering, this region is ignored because the total crack propagation life is not affected.

Therefore, the entire mechanism is operated in stage 2, where the Paris' law governs the larger magnitudes of ΔK. Whereas for smaller magnitudes, the plastic shear strain is governed. This represents the change from double shear continuum growth to single shear non-continuum growth [7]. da/dN (stage 2 in Fig. 5) is steady i.e., linear, which signifies good crystal structure, where the steep curve represents a sensitivity to microstructures and flow properties of the material [8]. In higher da/dN region, (stage 3 in Fig. 5) the values of k_{max} in N is tending towards K_{1C} and static modes of fracture are adding to the fatigue induced da/dN.

Given the complexity of the phenomena involved in different stages, there are no theoretical models available at present that can effectively take into account all the micro and macro mechanical aspects. However, Paris' law can be methodized even with little information provided the limitations are considered in crack phenomenon. Hence, Paris' law covers the da/dN ranges and extrapolation in the threshold region [9], which gives a cautious estimate for the life of the material. This is essential for the classical defect-tolerance concept to realize when to

IJASRM
International Journal of Advanced Scientific Research and Management, Volume 4 Issue 5, May 2019
www.ijasrm.com
ISSN 2455-6378

replace the damaged material i.e., capacity of the material over its demand.

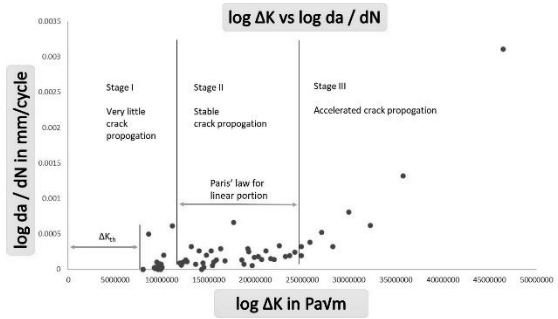

Fig. 5. Fatigue crack growth rate curve – log ΔK vs log da/dN

The fracture surface was observed under field emission gun (FEG) SEM after the experiment, where final striations and high dimples were observed signifying good breaking mechanism (Fig. 6.A). The fracture surface was mapped (Fig. 6.B) on FEG EDX to observe the distributions of plasma and polymer compounds upon material failure. In Fig. 6.B, the slightly darker region represents Al alloy and the darkest region represents the polymer compounds masking the plasma deposition. This signifies that the polymer layer breaks after the failure of the substrate. Therefore, polymers are suitable for protective coatings applications.

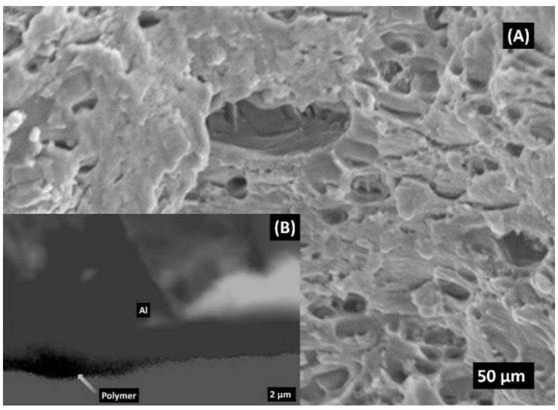

Fig. 6.(A). Fracture surface under FEG SEM and, (B). FEG EDX mapping on fracture surface

6. Conclusion

A new bio-based organic coating was synthesized with the aim of replacing paints in aeronautical industries for an eco-friendly environment. One of the advantages of such techniques are the possibilities on formulations by chemistry. This not only helps in obtaining desired mechanical or physio-chemical properties but also promotes plying similar to carbon fiber reinforced polymer composites, which can reduce the use of bulk materials. One of the interesting observations made in this work is that the behaviour of the composite is more similar to Al 2024 alloy synthesized by classical method i.e., cladding and anodization [10]. This signifies that neither plasma deposition nor polymer layer negatively influence the failure mechanisms of the metal. Therefore, the prospects of this research are parametric studies.

References

[1] Delebecq E, Pascault J.P, Boutevin B, Ganachaud F, On the versatility of urethane/urea bonds : Reversibility, blocked isocyanate, and non-isocyanate polyurethane. Chemical Reviews, 113(1): 80-118, (2012).

[2] Chattopadhyay D.K, Raju K.V.S.N, Structural engineering of polyurethane coatings for high performance applications. Progress in Polymer Science, 32(3): 352-418, (2007).

[3] Mertens J, Baneton J, Ozkan A, Pospisilova E, Nysten B, Delcorte A, Reniers F, Atmospheric pressure plasma polymerization of organics: effect of the presence and position of double bonds on polymerization mechanisms, plasma stability and coating chemistry. Thin Solid Films, 671: 64-76, (2019).

[4] Tryznowski M, Swiderska A, Zołek-Tryznowska Z, Gołofit T, Parzuchowski P.G, Facile route to multigram synthesis of environmentally friendly non-isocyanate polyurethanes. Polymer, 80: 228-236, (2015).

[5] Rosner H, Molenat G, Nembach E, In situ TEM observations of dislocation processes in iron-aluminides with 25 and 30 at.% aluminium. Materials Science and Engineering A, 216: 169-177, (1996).

[6] Paris P, Erdogan F, A critical analysis of crack propagation laws. Journal of Basic Engineering, 85(4): 528-534, (1963).

[7] Arunakumara P.C, Dinesh P, Fatigue crack growth study in polymer matrix composites. International journal of recent trends in engineering and research, 2(5): 284-289, (2016).

[8] Anderson T.L, Fracture mechanics, 4th Edition, CRC Press, Florida, 491-494, (2017).

[9] Grasso M, Iorio A.D, Xu Y, Haritos G, Mohin M, Chen Y.K, An Analytical Model for the Identification of the Threshold of Stress Intensity Factor Range for Crack Growth. Advances in Materials Science and Engineering, 3: 1-13, (2017).

[10] Mayer H, Schuller R, Fitzka M, Fatigue of 2024-T351 aluminium alloy at different load ratios up to 10^{10} cycles. International Journal of Fatigue, 27: 113-119, (2013).